REPORT DOCUMENTATION PAGE

Form Approved OMB No. 0704-0188

1. REPORT DATE *(DD-MM-YYYY)*	2. REPORT TYPE	3. DATES COVERED *(From – To)*
30-04-2009	Final Report	30 September 2005 - 24-Jun-09

4. TITLE AND SUBTITLE

Engineering Applications of Bird Flight

5a. CONTRACT NUMBER
FA8655-05-1-3077

5b. GRANT NUMBER

5c. PROGRAM ELEMENT NUMBER

6. AUTHOR(S)

Dr. Graham K Taylor

5d. PROJECT NUMBER

5d. TASK NUMBER

5e. WORK UNIT NUMBER

7. PERFORMING ORGANIZATION NAME(S) AND ADDRESS(ES)

University of Oxford
Tinbergen Building
South Parks Rd
Oxford OX1 3PS
United Kingdom

8. PERFORMING ORGANIZATION REPORT NUMBER

N/A

9. SPONSORING/MONITORING AGENCY NAME(S) AND ADDRESS(ES)

EOARD
Unit 4515 BOX 14
APO AE 09421

10. SPONSOR/MONITOR'S ACRONYM(S)

11. SPONSOR/MONITOR'S REPORT NUMBER(S)
Grant 05-3077

12. DISTRIBUTION/AVAILABILITY STATEMENT

Approved for public release; distribution is unlimited.

13. SUPPLEMENTARY NOTES

14. ABSTRACT

This report results from a contract tasking University of Oxford as follows: Description of Work:
We propose using a single common methodology to study wing morphing, automatic flow control, and vision-based guidance, navigation and control on free-flying birds. Eagles and other large birds of prey routinely carry loads comparable to their own body weight. Collaborative work by the BBC has already demonstrated that trained birds will fly carrying video cameras and telemetry systems weighing a few percent body mass. In-flight digital video has been obtained in this way from a variety of species in a variety of flight modes–from high-altitude soaring to flight through a cluttered woodland environment within a few feet of the ground. These existing data have already demonstrated a high degree of consistency in the manoeuvres executed by birds during obstacle avoidance, and most excitingly have revealed the existence of apparent automatic flow control devices in the wings of the birds, including a leading-edge flap which deploys automatically near the stall point.
We therefore propose to use calibrated stereo digital video to record the forward visual environment of the bird, the kinematics of the morphing wings, and the detailed movements of feathers involved in automatic flow control. These data will be complemented by heading, attitude, rate and acceleration data from an Inertial Measurement Unit (IMU), position data from a Global Positioning System (GPS), and airspeed data from a differential pressure transducer (DPT). Whereas the instrumentation will provide data for use in system identification of the flight control system, the onboard video cameras will be used to analyse automatic flow control devices in the wings and tail and to infer the contextual relevance of observed flight manoeuvres.
Trained birds of prey will also perform repeatable high-g intercept manoeuvres in attacking their handler's lure, and we will exploit this to obtain high-resolution high-speed digital video of approach and intercept manoeuvres, and also landing manoeuvres using ground-based cameras. These high-speed data will be essential in determining how the automatic flow control devices we identify are deployed in fast manoeuvres and through the course of a regular wingbeat.

Equipment & Facilities:
Animals: A variety of trained birds of prey are available locally from falconry enthusiasts.
Onboard digital video cameras: For the in-flight video recordings, we will use commercially available spy cameras in stereo configuration. High-resolution systems are now available at low cost with integral radio telemetry transmitters and lightweight battery packs. These cameras will be used for photogrammetric reconstruction of wing morphology using fiducial markers and for recording the deployment of automatic flow control devices. We will also use the onboard video to provide information on the visual and physical context of the mechanisms we record.
IMU, GPS, DPT: Recent advance in MEMS technology have enabled development of very small low-cost strap-down inertial navigation platforms. We will use an Xsens MTi platform, which is a miniature (50g) attitude and heading reference system that computes almost drift-free 3D orientation using rate gyros, accelerometers and magnetometers. Its low-power signal processor also provides calibrated 3D

acceleration, 3D rate of turn, and 3D earth-magnetic field data. To obtain position data (<3m accuracy) we will use a low-power Fastrax Upatch100 GPS receiver with integrated antenna (10g). Airspeed will be measured using a Sensortechnics HCXM100D6 DPT (5g). Seamless integration of these three sensors will be achieved using a PIC 16F877 microcontroller that will sample information from the three sensors and either store it on a multimedia memory card (through a built in SPI interface) and/or send it to a base station up to 900m away via a Maxstream 9Xtend radio modem (18g). The total weight to be included in the system is <110g, including battery, which constitutes <5% body mass for the species with which we will work.

High-speed digital video camera: High-speed video data will be essential for studying feather deployment in automatic flow control, owing to the high speed of attack manoeuvres and frequency of the wingbeat. To obtain high-speed digital video data in the field we will use a MotionScope M3, which records full frame (1280 by 1024 pixels) at 500 frames per second, with storage capacity for 2048 frames. The camera has a built-in rechargeable battery and is ruggedized for field use. In months 19-36 of the project, the purchase of a second M3 camera would allow us to use stereo videography to extract the 3D kinematics of the wingbeat and of wing morphing observed in avoidance manoeuvres.

Wind tunnel: A range of low-speed, low turbulence wind tunnels equipped with force transducers, flow visualisation facilities, etc. are available in the Zoology Department and Southwell Laboratories of Oxford University. These will be used to test models of the automatic flow control and wing morphing devices we identify.

Qualifications of Personnel:

Dr Graham Taylor (MA, D.Phil.) is a Royal Society University Research Fellow in the Department of Zoology, Oxford University, with expertise in animal flight dynamics and control. Dr Adrian Thomas (MA, PhD) is a University Lecturer in the Department of Zoology, Oxford University, with expertise in the aerodynamics of animal flight. Dr Marko Bacic (MEng, D.Phil.) is a University Lecturer in the Department of Engineering Science, Oxford University, with expertise in control engineering including system identification and inertial guidance platforms.

Schedule of Work:

Months 1-18: Outdoor experiments with free-flying birds. Months 1-3 will be needed to develop the camera and instrumentation systems. Months 4-12 will be used to collect and process data from free-flying birds, using onboard instrumentation, onboard digital video cameras and ground-based high-speed video cameras. Months 13-18 will be dedicated to analysing these data for: a) system identification of the flight dynamics, b) measurement of the morphology of morphing wings, c) identifying automatic flow control devices. Data will be passed to our collaborators in AFRL on a rolling basis. Interim reports will be supplied at the end of months 6 and 12, and a final report submitted at the end of month 18.

Months 19-36: Model validation, testing and refinement. A proposed extension to months 19-36 will be used to validate our models of the flight dynamics, and to test in the wind tunnel the effects of the automatic flow control devices and wing morphing mechanisms we identify. Additional outdoor experiments will be performed with birds to test predictions of the models we generate, using stereo high-speed video to analyse automatic flow control mechanisms and wing morphing kinematics in greater detail. Months 19-36 will enhance the collaboration with AFRL, offering the opportunity to answer questions about models of the flow control devices implemented on UAVs. Interim reports will be supplied at the end of months 24 and 30, and a final report submitted at the end of month 36.

15. SUBJECT TERMS

EOARD, Biotechnology, Aerodynamics, UAVs

16. SECURITY CLASSIFICATION OF:			**17. LIMITATION OF ABSTRACT**	**18, NUMBER OF PAGES**	**19a. NAME OF RESPONSIBLE PERSON**
a. REPORT	**b. ABSTRACT**	**c. THIS PAGE**			SURYA SURAMPUDI
UNCLAS	UNCLAS	UNCLAS	UL		**19b. TELEPHONE NUMBER** *(Include area code)* +44 (0)1895 616021

Engineering Applications of Bird Flight

Final Report on AFOSR Grant No. FA8655-05-1-3077

27 April 2009

Anna C. Carruthers, James Gillies, Yukie Ozawa, Simon M. Walker, Adrian L. R. Thomas and Graham K. Taylor[1]

Department of Zoology, South Parks Road, Oxford, OX1 3PS, United Kingdom

1. To whom correspondence should be addressed: graham.taylor@zoo.ox.ac.uk

1. Introduction

1.1 Summary of research

This report summarises the scientific content of the work undertaken under AFOSR Grant No. FA8655-05-1-3077. This research aimed to elucidate several aspects of bird flight, in order to identify potential technologies for transfer to the design of unmanned air vehicles (UAVs). Three areas for investigation were identified at the outset of the grant: wing morphing, automatic flow control, and vision-based guidance, navigation and control. This report describes results in each of these three areas. The techniques we use are novel, and the data we describe are therefore the first scientific data of their kind.

1.2 Summary of dissemination activities and outputs

The 5 published peer-reviewed journal papers and conference papers arising from this grant (Carruthers *et al*., 2007a,b; Gillies *et al*., 2008; Taylor *et al*., 2007a,b) are included as an electronic appendix to this report, together with a related conference paper on the low Reynolds number aerodynamics of leading-edge flaps (Bakhtian *et al*., 2007). Appendix I lists these publications together with all of the other research outputs of the grant. In total, we made 16 conference presentations, of which 2 were keynote presentations, and 9 appearances in the national or international media in the course of disseminating this research to the wider scientific community. Besides receiving regular visits from our sponsors at AFOSR (Dr Gregg Abate, Dr Johnny Evers) and other interested parties (Dr Michael Ol, Dr Rhett Jeffries), we also received visits from Air Force Chief Scientist Dr Mark Lewis in 2008, AFOSR Director Dr Brendan Godfrey in 2007, and AFRL Center of Excellence for Control Systems Director Dr Siva Banda in 2006. Finally, four members of the team made Windows on Science visits to Eglin AFB in 2005 and 2008.

2. Materials and methods

2.1 Animals

The research described in this report was undertaken with a trained male Steppe Eagle *Aquila nipalensis* (body mass: *c*. 2.5kg; typical chord Reynolds number: $Re=2\times10^5$) under the supervision of one or more trained handlers. The experimental protocol was approved by the United States Air Force, Surgeon General's Human and Animal Research Panel (SGHARP) for compliance with a) Title 9 Code of Federal Regulations, "Animals and Animal Products", chapter 1, subchapter A, "Animal Welfare", parts 1, 2, and 3; b) DOD Directive 3216.1, "Use of Laboratory Animals in DOD Programs, 17 April 1995, as amended; c) AFMAN 40-401, "The Care and Use of Laboratory Animals in DOD Programs", 1 December 2003 and d) The Guide for the Care and Use of Laboratory Animals - Institute of Laboratory Animal Resources, National Research Council, 1996. The experimental protocol was also evaluated by the Oxford University, Department of Zoology, Local Ethical Review Committee (LERC), and was considered not to pose any significant risk of causing pain, suffering, damage or lasting harm to the animal involved.

2.2 Onboard video

We have used a range of different wireless miniature video cameras and during the course of this research. The results described in this report are from 2.4GHz PAL CMOS cameras (Model 809, ZTV), with a total mass of 17g including battery (Carruthers *et al*., 2007a,b; Taylor *et al*., 2007a). Although these analogue video cameras are very reliable and allow recovery of deinterlaced video frames at 50Hz, problems with signal transmission when the bird is out of sight have lead us more recently to use a FlycamOne2 digital video camera (Acme OHG), with a total mass of 16g including battery (Gillies *et al.*, 2008). This logs 640×480 pixel digital video at 25Hz directly to an SD card for up to 40 minutes. In each case, the cameras are mounted on a removable harness made of webbing material and velcro straps, and can be positioned to look over the head, wings or tail. In total, we have obtained approximately 80 minutes of onboard video of the head, 10 minutes of onboard video of the wings, and 40 minutes of onboard video of the tail during wide-ranging free flight.

2.3 Onboard inertial instrumentation

We initially used an MTx/MTi (XSens Technologies B.V.) inertial measurement unit (IMU) together with an AntiLog data logger (Martelec Ltd) to record the bird's instantaneous 3D orientation, angular velocity and acceleration at an acquisition rate of 100Hz (Taylor *et al*., 2007a). This unit proved highly unreliable and we therefore switched to using a custom-built SmartIMU (Innovative Automation Technologies, LLC) with integrated data logger (Gillies *et al.*, 2008). The unit has a total mass of 104g including battery, and measures 100×50×35mm. The SmartIMU measures three-axis orientation, rotation rate and linear acceleration at 25Hz, and 3-axis velocity and position at 6Hz, using a combination of magnetometers, rate gyros, linear accelerometers, and GPS location and GPS Doppler shift. The instrumentation was carried on the eagle's back, worn on a removable harness made of webbing material and velcro straps.

During the course of the grant, the bird has been flown freely at a range of field sites in Wales, yielding approximately 3h of flight data to date, of which approximately 40 minutes is accompanied by onboard video of the tail (see Section 2.2).

Because the position and orientation of the IMU with respect to the bird is unknown, all measurements need to be transformed into a meaningful frame of reference prior to analysis. This was achieved through a series of coordinate transformations (Gillies *et al.*, 2008), which made use of the statistical properties of each flight to transform all measurements made in the IMU frame of reference (FI) into a suitable body frame of reference (FB). The directions of the axes of FB were fixed by aligning the x_{FB}-axis with the mean direction of flight in FI, and by aligning the y_{FB}-axis with the plane of the horizontal in FI. The rotated frame of reference was then translated so that its origin coincided with the mean centre of mass of the bird, by making use of the measurements of acceleration and angular velocity. The acceleration $\hat{\boldsymbol{a}}=[\hat{a}_x, \hat{a}_y, \hat{a}_z]$ sensed at an arbitrary point $\mathbf{P}=[x, y, z]$ is related to the acceleration $\boldsymbol{a}=[a_x, a_y, a_z]$ at the centre of mass $\mathbf{O}=[0, 0, 0]$ by the equations:

$$\begin{aligned}
\hat{a}_x &= a_x - \left(r^2 + q^2\right)x + \left(-\dot{r} + pq\right)y + \left(\dot{q} + pr\right)z \\
\hat{a}_y &= a_y + \left(\dot{r} + pq\right)x - \left(r^2 + p^2\right)y + \left(-\dot{p} + qr\right)z \\
\hat{a}_z &= a_z + \left(-\dot{q} + pr\right)x + \left(\dot{p} + qr\right)y - \left(p^2 + q^2\right)z
\end{aligned} \qquad \text{(Equation 1)}$$

where $[p, q, r]$ are the components of angular velocity in an inertial frame of reference. These equations are linear in the unknown coordinates $[x, y, z]$ of the sensor so the least squares solution of these equations gives an unbiased estimate of $[x, y, z]$, and hence of the position of the IMU relative to the centre of mass of the bird. This was used to fix the origin of FB at the centre of mass. On the assumption that flight consists of symmetric perturbations from equilibrium, FB approximates a stability axis system (i.e. with the x- and z-axes in the symmetry plane, and the x-axis directed parallel to the equilibrium line of flight, such that the pitch angle is zero at equilibrium).

2.4 High-speed videography and photogrammetry

Flight tests using one or two high-speed digital video cameras (Motionscope M3, Redlake Inc.) were conducted in a large open field (Fuglslev, Djursland: 13-15 March, 2006 and 18-23 October 2006; Abergavenny, Wales: 18-22 June 2007) and indoors in a 30m long enclosed barn. In total, we have recorded 37 separate perching sequences for this part of the study, comprising 23 outdoor and 14 indoor sequences (Carruthers *et al.*, 2007b). The cameras recorded up to 4096 monochrome 1024×1280 pixel images at 500fps with a shutter time of 0.002s, giving *c*. 4s of recording time. Flying the bird in still air in a confined space indoors allowed us to elicit quite different flight behaviours during perching from those elicited outdoors when the bird landed in a headwind of between 1.5 and 6.7ms^{-1}. Specifically, whereas the eagle typically

used a gliding landing approach outdoors, all indoor flights involved a flapping landing approach.

Although we primarily used our high-speed video data to identify wing morphing and feather deflection (Carruthers *et al*., 2007b), we also used high-speed photogrammetry to identify the gross kinematics of a single wingbeat (Carruthers *et al*., 2007a). The cameras were calibrated using a 2D calibration grid of known size and structure, which was filmed in multiple positions and orientations throughout the measurement volume. We used custom-written software to locate points on the calibration grid semi-automatically, and used a nonlinear least squares algorithm to perform a bundle adjustment which provided jointly optimized estimates of the camera calibration parameters and spatial coordinates of the grid points. We then used the camera calibration to estimate the spatial coordinates of *c*. 70 points on the wings and body, identified manually using natural markers, such as feather tips and pigmentation (Figure 1).

2.5 High-resolution photogrammetry

High-resolution (3504×2336 pixel) images of the wings were collected during perching manoeuvres using six digital SLR cameras (Canon EOS 30D) synchronised to within 1 or 2ms (see Figure 2). Up to 5 sets of 6 frames were recorded for a given manoeuvre, and stereo high-speed video (Section 2.4) of the manoeuvre was also recorded to provide context for the sequence. Although we recorded both flapping and gliding perching sequences, the results we describe are for a single gliding sequence only. The cameras were calibrated using the same bundle adjustment technique as for the high-speed video (Section 2.4). We then used the camera calibration to estimate the spatial coordinates of 380 points on the wings, identified manually using natural markers, such as feather tips and pigmentation.

3. Results

3.1 Use of wing morphing and variable tail geometry in manoeuvres

The eagle routinely uses five highly stereotyped manoeuvres in flight (Gillies *et al*., 2008), of which all but the banked turn involve extensive use of wing morphing and changes in tail geometry:

Banked turns. Most turns in soaring flight are banked turns, and we have made inertial measurements of over 100 such turns in which the bird rotated >45˚ in azimuth. Banking is initiated by increasing the angle of attack of the outside wing relative to the inside wing, which produces a roll moment into the turn (Figure 3). Roll into the turn is checked by an opposite change in the relative angles of attack. Roll back into level flight is initiated by an increase in the angle of attack of the inside wing relative to the outside wing, and is again checked by an opposite change in the relative angles of attack. These changes in wing angle of attack are accompanied by a pair of step-changes in the bank of the tail relative to the body during roll into and roll out of the turn. These were

measured from the onboard video of the tail, and are visible in Figure 4, which plots inertial data and tail kinematics for a typical banked turn.

Wing tucks. A second common and stereotyped manoeuvre is the wing-tuck, and we have recorded inertial measurements of 128 such manoeuvres. The frequency of tucks is not increased by carrying equipment, but appears to be positively correlated with wind speed (Figure 5), suggesting that the tuck might be a form of gust response. During a typical tuck, the eagle pulls his wings down together and holds them there momentarily. The tail is spread simultaneously, and then lifted sharply as the wings reach their maximum excursion. The wings are then raised and spread fully, and soaring is restored. The time elapsed between the beginning of the wings' downward motion and their spreading at the end of the manoeuvre is typically only 0.25s. Tucks are associated with a characteristic pattern of inertial acceleration (Figure 6), which approaches 1g as the bird enters effective freefall with the wings closed, and is followed by a period of high negative acceleration in the z_{FB}-axis as the wings are spread. The dropping of the wings also results in a rapid nose-down pitching motion, which is subsequently counteracted by the lifting of the tail, which limits the amplitude of the nose-down pitching motion to <30°. The resulting dive causes the bird to gain forward airspeed, via a rapid exchange of potential and kinetic energy.

Stoops. When the eagle intends to lose altitude rapidly – for example, when called in by the handler, he initiates a stoop. We have observed over 30 such manoeuvres, and have obtained inertial measurements of 3. Stoops are initiated by a partial wing tuck, after which the wings are swept forwards into an M-shaped planform. This reduces lift and drag, and allows higher speeds to be reached. The bird then rolls through >90°, which initiates a sideslip that is checked by yawing into the direction of the sideslip and then rolling back into a steep level dive. As the bird approaches the ground, he decelerates rapidly by pulsing the angle of attack of his wings, so that they alternately enter and recover from stall. Increases in wing angle of attack are closely phased with spreading and lowering of the tail, which counteracts the large pitching moment that would otherwise result.

Perching. The final stages of perching are described in detail in one of the appended papers (Carruthers *et al*., 2007b), based on high-speed video of 37 landing sequences. A typical perching sequence involves three sequential phases: a shallow approach, a rapid pitch-up manoeuvre, and a deep stall (Figure 7). The approach phase usually involves a glide in ground effect with the wings fully outstretched, and ends with the bird well below the level of the perch. The bird then executes a rapid pitch-up manoeuvre by sweeping its wings forward into an M-shape and tilting the tail up. The bird's kinetic energy is reduced by as much as 30% during this phase of the manoeuvre as the bird gains height and potential energy. Towards the end of the pitch-up manoeuvre, the wings and tail are spread fully and the tail is tilted down. The angle of attack of the wings at this stage of the manoeuvre approaches 90˚ and the upperwing exhibits massive feather deflection, indicative of separation over the entire suction surface of the arm wing. Flapping perching sequences end in a similar fashion, also ending with a pitch-up manoeuvre and deep stall.

Inversions. We have recorded inertial measurements of 7 instances in which the bird inverted as a response to mobbing by other birds. This is a complicated manoeuvre involving extensive morphing of the wings. A rapid roll is initiated by decreasing the angle of attack of the leading wing, and rotating it so that the tip points down. As the body rolls past 90°, the outside wing is folded into the body. Roll back out of the inversion is initiated by re-opening the outside wing. Both wings are then spread horizontally as the bird returns to level flight.

3.2 Automatic aeroelastic devices

The gross active changes in wing morphology described in Section 3.1 are accompanied by much finer changes in wing structure due to passive feather deflection. Deflections of the upperwing covert feathers accompany flow separation and tend to be rather chaotic. For this reason, we do not describe them further here, although it is possible they play a role in limiting the extent of separation (Carruthers *et al*., 2007b). Instead, we focus upon deflection of the lesser underwing coverts (i.e. the rows of feathers immediately beneath the leading edge of the inner wing) and of the alula (i.e. the group of feathers positioned on the thumb remnant at the primary flexion point of the wing leading edge). These are described in detail in Carruthers *et al*. (2007b).

Mass deployment of the lesser underwing coverts was observed on all 24 landing sequences and all 6 flapping take-off sequences recorded using the onboard cameras. We also observed their deployment on 33 of the 37 perching sequences taken using the high-speed cameras, and during 5 single wingbeats that interrupted soaring flight. In addition to these deployments in landing manoeuvres and flapping, we observed 2 instances of underwing covert deployment during 2 separate bouts of soaring as the bird flew low over the cliff edge, which must have been associated with a significant updraft given the strong onshore breeze. Deployment of the lesser underwing coverts appears to be a passive phenomenon, which occurs automatically at high angle of attack, as the forward stagnation line moves behind the tips of the feathers. The resulting locally reversed flow lifts the feathers away from the surface of the wing. This produces a flap-like structure reminiscent of a Kruger flap, which can be deployed as a single unit or in sections according to the local flow conditions.

Protraction of the alula was observed on most landing sequences. Although protraction is an active phenomenon under muscular control, the alula first begins to peel upwards at its tip. This indicates that the alula is lifted passively from the wing surface during the initial stages of its deployment, as the muscles attach at the base of the feathers. Active protraction of the alula from its base could only be seen after passive peeling from the tip had occurred Deployment of the alula is therefore a two-stage process, and we speculate that the second, active stage may be initiated by the first, passive stage via a positive feedback mechanism. In any case, the alula deploys fully during landing sequences at the point at which the wing is swept maximally forward. The resulting M-shaped planform means that each wing is likely to act, in effect, as a delta wing, and we think it likely therefore that the alula is acting as a strake, serving to promote and stabilise the formation of a leading-edge vortex over the

swept portion of wing behind it. We note that this interpretation differs markedly from the classical description of the alula as a leading-edge slot or slat (e.g. Nachtigall & Kempf, 1971).

3.3 Wing shape and aerodynamics

The airfoil sections of birds differ substantially from most technical airfoils. Experimental or numerical tests of the aerodynamic function of the automatic aeroelastic devices outlined in Section 3.2 are only likely to make sense if the airfoil section used is a realistic one, and we therefore used our photogrammetric measurements to reconstruct the shape of the inner wing at one representative point in a perching sequence. The wing deforms markedly under load, and the airfoil section we derive should therefore be taken as a representative example of a family of airfoils, rather than as a unique and general representation of the eagle's wing.

The wing surface was modelled using multiple regression, fitting the upper and lower surfaces of the inner wing separately. The regressions model that we used fitted a constant airfoil section of varying chord, angle of incidence and elevation along the span. The shape of each airfoil surface was well modelled as a third order polynomial in the distance from the leading edge, while spanwise bending was well modelled by a fourth order polynomial in the distance from the wing root. Angle of incidence was well modelled by a linear twist distribution along the wing. The fitted upper and lower surfaces do not quite meet at the leading edge, owing to the low order of the polynomials used, so a Bezier function was used to join the two. The trailing edge of the wing was given a 1mm thickness, based on measurements of the eagle's feathers. Figure 8 plots the fitted surface. The airfoil itself (Figure 9) has a very high degree of camber and in this respect resembles technical airfoils engineered to generate high-lift at low Reynolds number (e.g. the Selig 1223). Airspeed and angle of attack were measured from the high-speed video using stereo photogrammetric techniques and anemometric measurements.

As a first step towards assessing the aerodynamic properties of the wing (see Section 5 for future work), we used Javafoil to predict lift and drag coefficients at low angles of attack. Javafoil uses a high order panel method to calculate the velocity along the aerofoil surface. Beginning at the leading edge stagnation point, the boundary layer is then evaluated over upper and lower surfaces for transition and separation. The program does not model either laminar separation bubbles or flow separation and assumes inviscid flow. It is therefore likely to provide reasonable results at low angle of attack, but to become inaccurate at the onset of separation. The results plotted in Figure 9 should therefore only be judged reliable in the approximate range $0<\alpha<8^{\circ}$. The predicted lift coefficients reach approximately $C_L=1.5$ over this range, which is reasonable, but nowhere near matching technical airfoils such as the Selig S1223 at comparable chord Reynolds numbers.

3.4 Head movements

The final part of this project considered aspects of vision-based guidance, navigation and control (Taylor *et al*., 2007a). Birds rely heavily upon vision, and the central problem that this poses is that of motion blur during manoeuvres. In mammals, motion blur is avoided by way of fast saccadic eye movements. In a bird such as the Steppe Eagle, however, the eyes have relatively little freedom of movement and large gaze shifts are therefore effected by movements of the head. We analysed the role of saccadic head movements during banked turns using onboard video (Taylor *et al*., 2007a). Head saccades about the yaw axis were found to be strongly associated with banked turns (166 saccades expected during turns based on Poisson distribution, compared to 516 observed, $p<0.00001$). Where saccades and turns were associated, they were found to agree strongly in their direction (exact binomial test: $p<0.00001$, $n=514$). Although several saccades could be associated with a single turn, the first saccade of a turn always began at or before the onset of the turn, indicating that the saccade is commanded in an open-loop fashion during voluntary turns. This differs from the pattern observed during gaze stabilization in response to imposed involuntary turns, in which the saccade is a closed-loop response to the rotation.

The overall pattern was one of nystagmic gaze stabilization in which short saccadic head movements were used to achieve longer periods of gaze fixation during which the head maintained a constant orientation with respect to the Earth (Figure 20). Nystagmic gaze stabilization is likely to be important in preventing motion blur, but may also be important in disambiguating the input from the part of the vestibular system sensing linear accelerations. Equation 1 above shows that the linear acceleration sensed at a point removed from the centre of mass of a body is different from the linear acceleration of the centre of mass unless all of the angular velocities and accelerations are zero. During periods of gaze fixation, the orientation of the head remains constant in inertial space, and it follows, therefore, that the vestibular system in the head will be able reliably to measure the linear acceleration of the body.

4. Conclusions

The conclusions of this research are expanded upon at length in the appended published papers and conference papers (Carruthers *et al*., 2007a,b; Gillies *et al*., 2008; Taylor *et al*., 2007a,b). Here we attempt only to point to those areas which we consider to be most relevant in technology transfer to UAVs.

The aerodynamic function of the lesser underwing coverts remains uncertain (see Carruthers et al., 2007b). It is possible that they act as a leading-edge flap delaying the onset of stall, and we are currently investigating this possibility (see Section 5). In any case, since every feather follicle is associated with sensory neurons, it is reasonable to assume that the bird has available to it information on the deflection of the feathers (Brown & Fedde, 1993). It follows that the lesser underwing coverts could be used as a distributed sensor to detect local incipient stall. This ability to detect local flow conditions could be of

particular use in the unsteady and localised flow conditions that we expect to be associated with morphing-wing UAVs.

Wing morphing is clearly central to controlling flight manoeuvres in our eagle, but it is striking that wing morphing is usually accompanied by changes in tail geometry. The variable geometry of the tail appears to be of particular importance in counteracting the unsteady pitching motions that would otherwise result from changing the area and planform of the wings. It is reasonable to assume that morphing-wing UAVs will require similar compensation in tail shape, orientation and area if they are to effect successful manoeuvres. Our results provide some insight into possible ways in which wing morphing and changes in tail geometry could be phased.

The movements of the tail are of particular interest to UAV design, since the bird lacks a vertical tail, and thereby avoids the weight and drag penalty associated with having one. We are currently investigating the function of the horizontal tail in compensating for adverse yaw during banked turns, and it is likely that a similar tail design (i.e. a triangular tail with two degrees of freedom of rotation and variable spread) could find use in a fixed-wing UAV where payload is limited by the weight of the airframe.

5. Current directions

The pilot work enabled by this grant was instrumental in allowing one of us (GKT) to secure a grant of €1.95M from the European Research Council under the European Community's Seventh Framework Programme (ERC Grant Agreement no. 204513). Part of the work under this new grant will use system identification techniques to model the function of wing morphing, variable tail geometry, and automatic aeroelastic devices in the flight of the Steppe Eagle. Although we had originally hoped to use system identification in the course of the present grant, this did not prove possible owing to technical limitations of the onboard equipment we used. These will be overcome in the next generation of SmartIMU, which we have commissioned Innovative Automation Technologies to produce. The new IMU will measure airspeed, angle of attack and sideslip angle in addition to the inertial measurements we have already made, thereby providing us with the necessary and previously missing information on airflow.

The remaining 18 months of JG's PhD will involve using 3-axis measurements of airspeed made with a new ultrasonic anemometer to investigate the gust response and glide polar of the eagle, as determined from inertial measurements made simultaneously as the bird hangs in an updraft at the handler's first. This builds upon pilot work undertaken in April 2009 with Simon Watkins (RMIT) using multi-hole pressure probes (Turbulent Flow Instrumentation Pty Ltd.) to resolve 3 components of velocity and local static pressure at four closely-spaced points close to where the eagle was flying. Related research will test the hypothesis that wing tucks represent a form of gust response, which we speculate is used to recover a well-behaved attached flow.

The remaining 6 months of ACC's Royal Commission for the Exhibition of 1851 Research Fellowship will be spent analysing the aerodynamic properties of the eagle's airfoil section and the function of the leading-edge flap. This wing section is currently being analysed using a commercial CFD package (Fluent). Future numerical work will incorporate a leading-edge flap and will compare the eagle's airfoil performance to a technical low Reynolds number aerofoil (Selig S1223). Wind tunnel tests of the airfoil section are still planned, but have had to be postponed for a number of reasons, including rewiring of the REEF wind tunnel facility force balance and changes to the airfoil section. Other suggested work would involve implementing the same airfoil-flap configuration on a fixed-wing UAV such as the GENMAV.

6. Proposed future work

ALRT has recently applied for BBSRC funding to examine the use of morphing wings in birds. The proposed work will use the photogrammetric techniques developed here, applied to birds executing glides and dives at a wide range of speeds, during steady banked turns at high-G, and during the initiation and termination of manoeuvres (pitch down, pitch up, turn entry, turn exit). The project will provide detailed 3D models of the wing, body and tail morphologies the birds select for steady slow glides, high-speed dives, and steady turns as well as during dynamic manoeuvres. These models will form the basis of future CFD analyses of bird flight designs.

Separately, GKT and ALRT are in discussions with Dr Gregg Abate in relation to a proposed new effort to implement some of the features described above on a remote-controlled air vehicle. This effort would use wind tunnel tests for initial parameter estimation and onboard inertial instrumentation for system identification analysis of control systems and automatic flow control devices inspired by those used by the Eagle. This builds upon the insight that a remote-controlled "bird" with a realistically-actuated horizontal tail and fixed wings with ailerons behaves in a similar fashion to a real bird, requiring in particular a similar phasing of control inputs to effect manoeuvres. A white paper outlining the proposed effort in more detail is forthcoming.

Acknowledgments

We thank Gregg Abate, Johnny Evers and Michael Ol for their close involvement and support of the work under this grant. We thank Surya Surampudi for the assistance he has provided at EOARD. We thank Simon Watkins and Mark Thompson for their cooperation in making turbulence measurements. We thank Holger Babinsky and Noel Bakhtian for their useful input in the early stages of this grant, and thank Fran Yuan for advice on system identification. Marco Bacic was instrumental in the early stages of the inertial measurements. We gratefully acknowledge the assistance of our bird handlers Louise Crandal, Martin Cray and Jo Binns, and thank our Steppe Eagle "Cossack" for his assistance throughout. ACC was supported by a Royal Commission for the

Exhibition of 1851 Research Fellowship. GKT was supported by a Royal Society University Research Fellowship and RCUK Academic Fellowship.

References

Bakhtian, N. M., Babinsky, H., Thomas, A. L. R. and Taylor, G. K. (2007). The low Reynolds number aerodynamics of leading edge flaps. *AIAA-2007-662.*

Brown, R.E. and Fedde, M.R. (1993) Airflow Sensors in the Avian Wing. *J. Exp. Biol.* **179**: 13-30.

Carruthers, A. C., Thomas, A. L. R. & Taylor, G. K. (2007a). Use and Function of a Leading Edge Flap on the Wings of Eagles. *AIAA 2007-43.*

Carruthers, A. C., Thomas, A. L. R. & Taylor, G. K. (2007b). Automatic aeroelastic devices in the wings of a Steppe Eagle *Aquila nipalensis*. *J. Exp. Biol*. **210**, 4136-4149

Gillies, J., Bacic, M., Yuan, F. G., Thomas, A. L. R., and Taylor, G. K. (2008). Modeling and Identification of Steppe Eagle (*Aquila nipalensis*) dynamics. *AIAA-2008-7096.*

Nachtigall, W. and Kempf, B. (1971) Vergleichende Untersuchungen zur Flugbiologischen Function des Daumenfittichs (Alula spuria) bei Vogeln, *Z. Vergl. Physiologie* **71**: 326-341.

Taylor, G. K., Bacic, M., Carruthers, A. C., Gillies, J., Ozawa, Y. and Thomas, A. L. R. (2007a). Flight control mechanisms in birds of prey. *AIAA-2007-39*.

Taylor, G. K., Bacic, M., Bomphrey, R. J., Carruthers, A. C., Gillies, J., Walker, S. M. and Thomas, A. L. R. (2007b). New experimental approaches to the biology of flight control systems. *J. Exp. Biol.* **211**: 258-266.

Appendix I - Research Outputs

Peer-reviewed journal papers

[1] Carruthers, A. C., Thomas, A. L. R. & Taylor, G. K. (2007b). Automatic aeroelastic devices in the wings of a Steppe Eagle *Aquila nipalensis*. *J. Exp. Biol*. 210, 4136-4149

[2] Taylor, G. K., Bacic, M., Bomphrey, R. J., Carruthers, A. C., Gillies, J., Walker, S. M. and Thomas, A. L. R. (2007b). New experimental approaches to the biology of flight control systems. *J. Exp. Biol.* 211: 258-266.

Published conference papers

[1] Bakhtian, N. M., Babinsky, H., Thomas, A. L. R. and Taylor, G. K. (2007). The low Reynolds number aerodynamics of leading edge flaps. *AIAA-2007-662.*

[2] Carruthers, A. C., Thomas, A. L. R. & Taylor, G. K. (2007a). Use and Function of a Leading Edge Flap on the Wings of Eagles. *AIAA 2007-43.*

[3] Gillies, J., Bacic, M., Yuan, F. G., Thomas, A. L. R., and Taylor, G. K. (2008). Modeling and Identification of Steppe Eagle (*Aquila nipalensis*) dynamics. *AIAA-2008-7096.*

[4] Taylor, G. K., Bacic, M., Carruthers, A. C., Gillies, J., Ozawa, Y. and Thomas, A. L. R. (2007a). Flight control mechanisms in birds of prey. *AIAA-2007-39*.

Keynote presentations at international meetings

[1] Aerodynamics and control of free-flying birds of prey. G. Taylor. DFG SPP-1207 (Nature Inspired Fluid Mechanics) Annual Colloquium, Darmstadt, Germany, 8-9 October 2007.

[2] *Flying with flexible wings: lessons from birds and insects*. G. Taylor. Bionique network (CNRS RTP) meeting. Tours, France, 15 January 2009.

Invited oral presentations at international conferences

[1] Free-flight aerodynamics of birds from onboard cameras and instrumentation. A. Thomas, G. Taylor, A. Carruthers. Society for Experimental Biology, Annual Main Meeting, Canterbury, UK, 2-7 April 2006

[2] System identification of avian flight dynamics and control. G. Taylor, Y. Ozawa. Society for Experimental Biology, Annual Main Meeting, Canterbury, UK, 2-7 April 2006

[3] Biologically-Inspired Flight for Micro Air Vehicles, AFOSR Workshop, Denver, CO, USA, 21-23 June 2006.

[4] New experimental approaches to the biology of flight control systems. G. Taylor. 5th World Congress of Biomechanics. Munich, Germany, 29-4 August 2006.

[5] Vision-based flight control in birds and insects. G. Taylor. Applied Vision Association Colour Group Meeting, London, UK, 20 September 2007.

[6] Bird wing aerofoil sections and control devices for MAV application. A. Carruthers, A. Thomas, S. Walker, J. Gillies, G. Taylor. 24th Bristol International UAV systems conference 30 March – 1 April 2009

Contributed oral presentations at international conferences

[1] Onboard video in free-flight analysis of birds; use of head and eyes in vision-based flight control

Y. Ozawa, G. Taylor. Society for Experimental Biology, Annual Main Meeting, Glasgow, UK, 31 March - 4 April 2007

[2] Aeroelastic control devices and wing kinematics of a Steppe eagle *Aquila nipalensis* during perching manoeuvres. A. Carruthers, A. Thomas, S. Walker, G. Taylor Society for Experimental Biology, Annual Main Meeting, Glasgow, UK, 31 March - 4 April 2007

[3] Flow control in the wings of a Steppe eagle *Aquila nipalensis*: automatic aeroelastic devices

A. Carruthers, A. Thomas, G. Taylor. Society for Experimental Biology, Annual Main Meeting, Marseille, France, 6-10 July 2008

Poster presentations at international conferences

[1] Onboard Video for free-flight analysis of vision-based flight control in birds. Y. Ozawa, G. Taylor, Society for Experimental Biology, Annual Main Meeting, Canterbury, UK, 2-7 April 2006

[2] Identification of the flight control system of the Steppe eagle *Aquila nipalensis*. Gillies, A. Thomas, G. Taylor, M. Bacic. Society for Experimental Biology, Annual Main Meeting, Glasgow, 31 March - 4 April 2007

Media coverage

[1] Discovery Channel, *Daily Planet*. (2006) News interview on bird flight research.

[2] German Public Radio. (2006) News interview on bird flight research.

[3] Eagle wings deploy leading edge flaps (2007) *Journal of Experimental Biology* 210, pp ii

[4] Secret of Eagles' Landing Revealed (2007) *New Scientist*, Issue 2599 pp19, 16 April

[5] Discovery Channel, *Modern Marvels* (2007).

[6] Atmospheric Flight Mechanics (2007) *Aerospace America*, December 2007.

[7] BBC Radio Online, Naked Scientists. (2007). News interview on animal flight research.

[8] ARD German Television, *[W] wie Wissen* (2008). Documentary interview on flocking flight dynamics.

[9] National Geographic Channel. *Richard Hammond's Engineering Connections: Super Jumbo – A380* (2008).

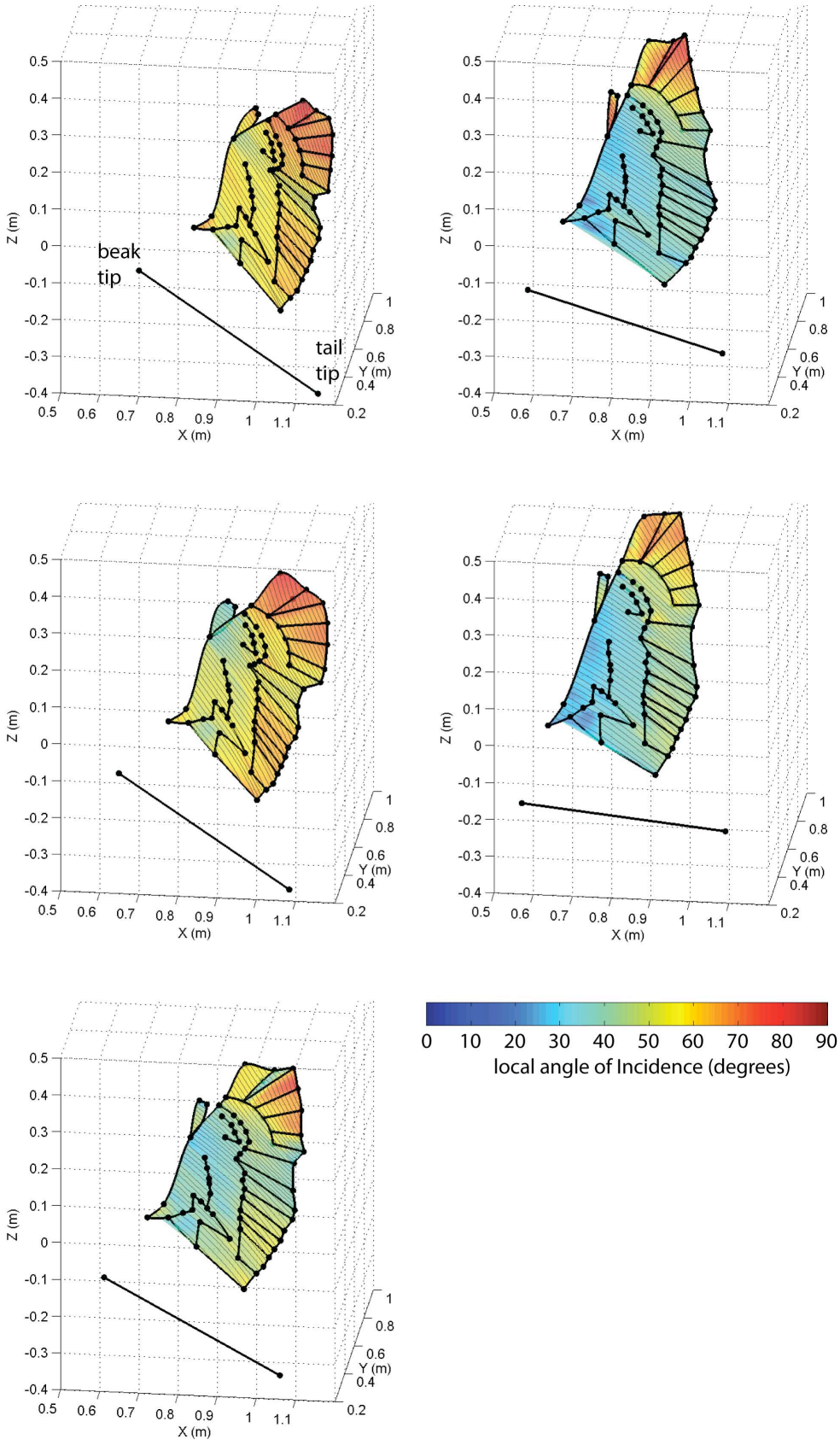

Figure 1. Photogrammetric reconstruction of the kinematics of a single wingbeat during a flapping perching sequence.

Figure 2. High-resolution (3504×2336 pixel) images of the wings were collected during perching manoeuvres using six digital SLR cameras (Canon EOS 30D) synchronised to within 1 or 2ms.

Figure 3. Simultaneous ground-based and onboard video of a banked turn, showing the use of the tail to counteract adverse yaw (compare the bank of the tail in the frames at 45.5 and 46.0s, to its opposite bank in the frames at 48.0 and 48.5s).

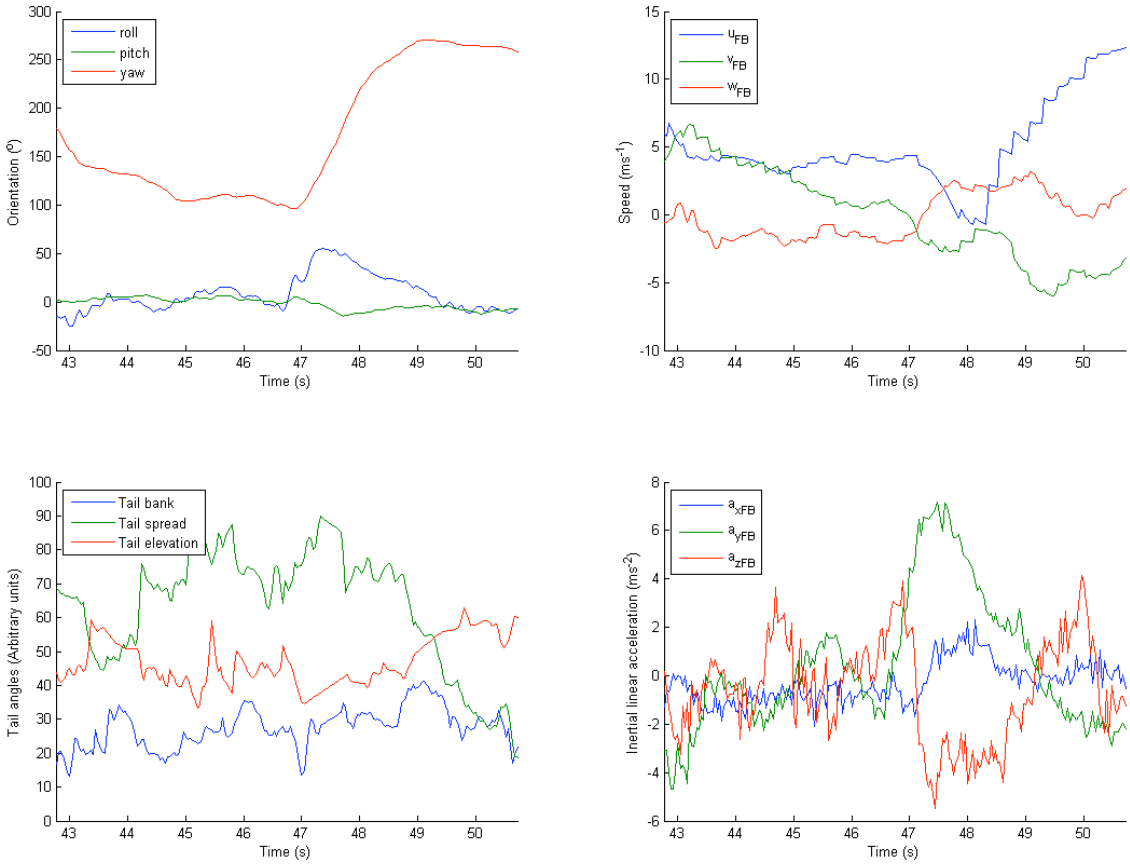

Figure 4. Inertial data (azimuth; ground speed; linear acceleration) and tail kinematics (tail bank, spread and elevation) during a typical banked turn.

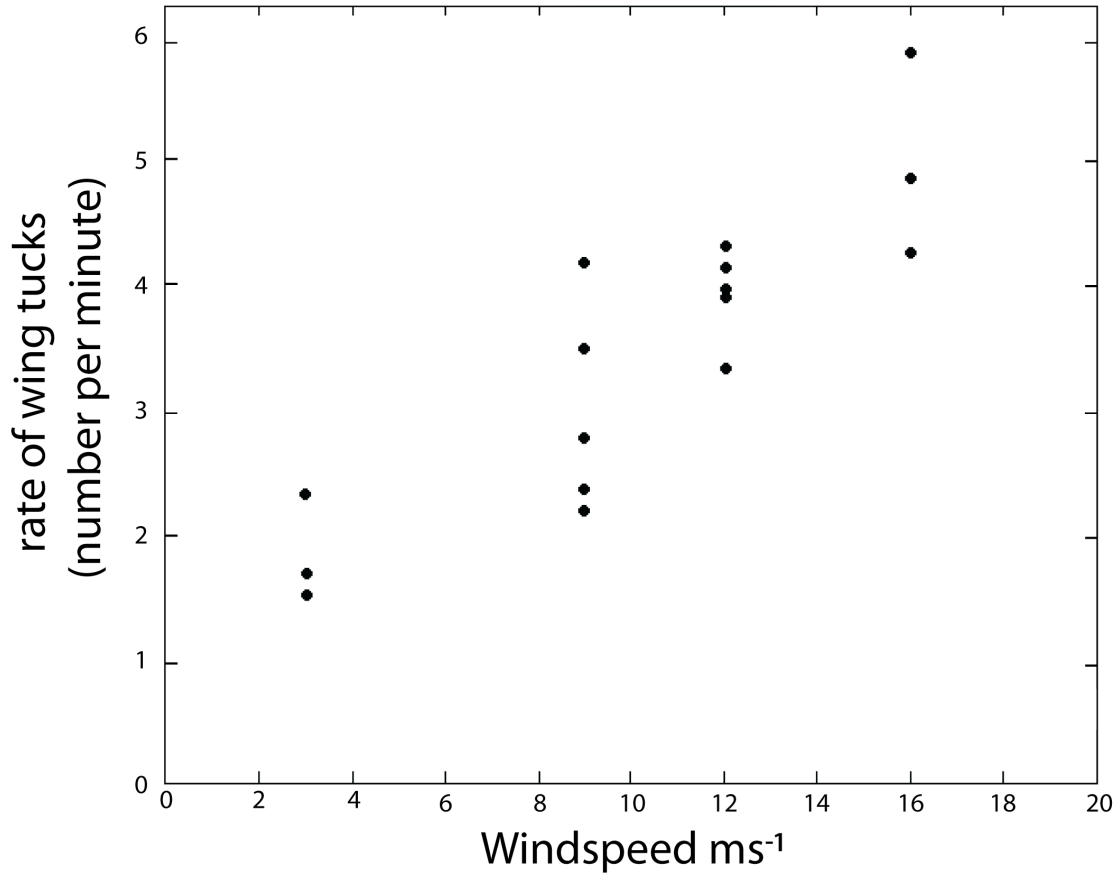

Figure 5. Graph showing rate of wing tuck occurrence (number of tucks observed per minute) against wind speed for 16 flights in the Abergavenny area during June and July 2008.

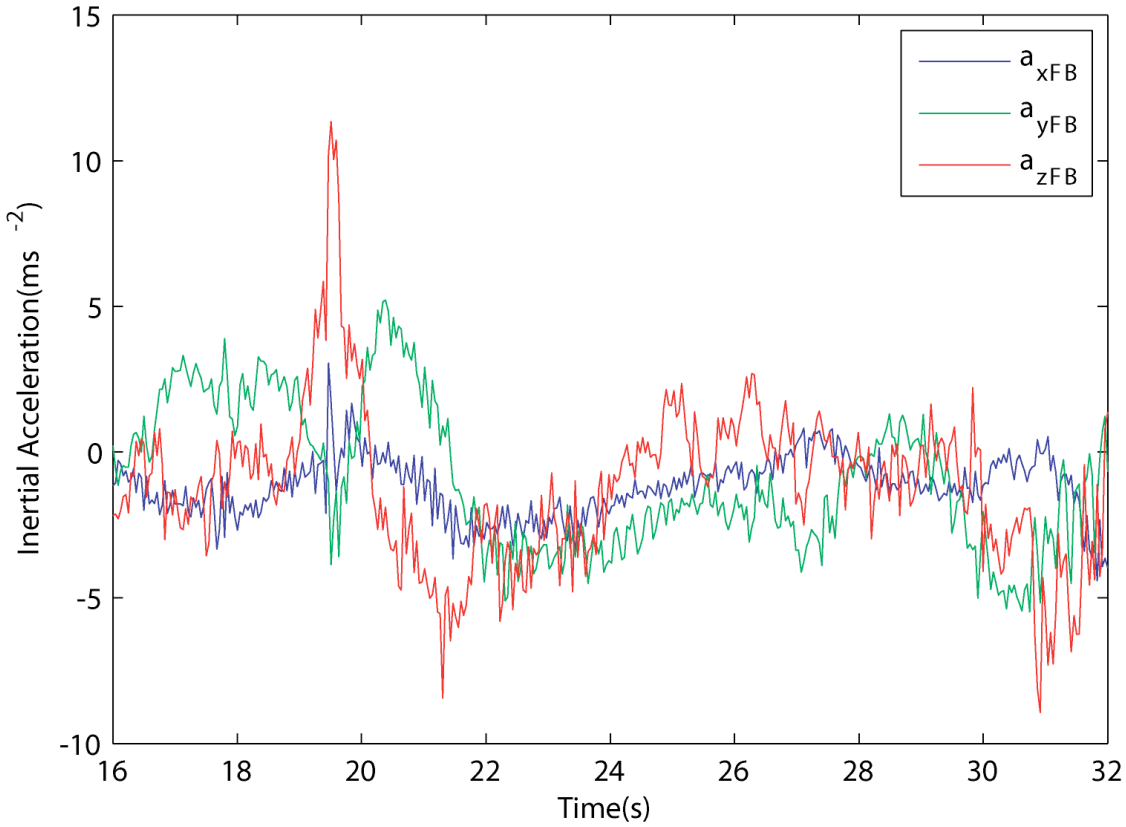

Figure 6. The characteristic pattern of inertial acceleration seen during a typical wing tuck.

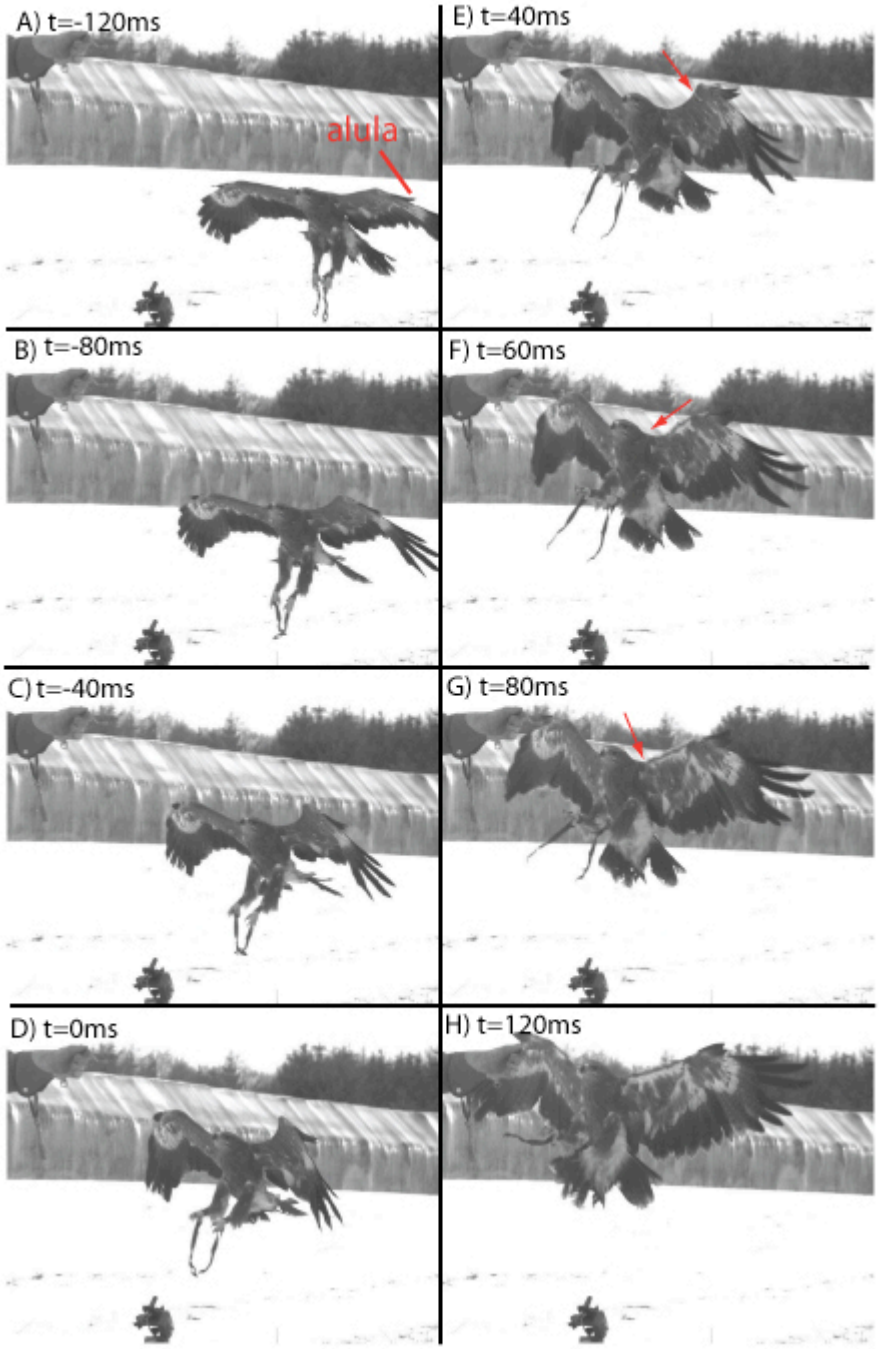

Figure. 7. Gliding perching sequence. Phase 1: gliding approach: (A) Alula begins to peel upwards; tail flicked up and back. Phase 2: pitch-up manoeuvre. (B-D) Wrist sweeps forward. (E) lesser underwing coverts begin to deflect from wrist (red arrow); alula starts to protract; wing begins to straighten; tail spreads and pushes downwards and forwards. (F) Lesser underwing coverts deflecting in travelling wave from wrist towards shoulder (red arrow). (G) Lesser underwing coverts fully deflected (red arrow). Phase 3: deep stall. (H) Wings outstretched to give parachute-like shape.

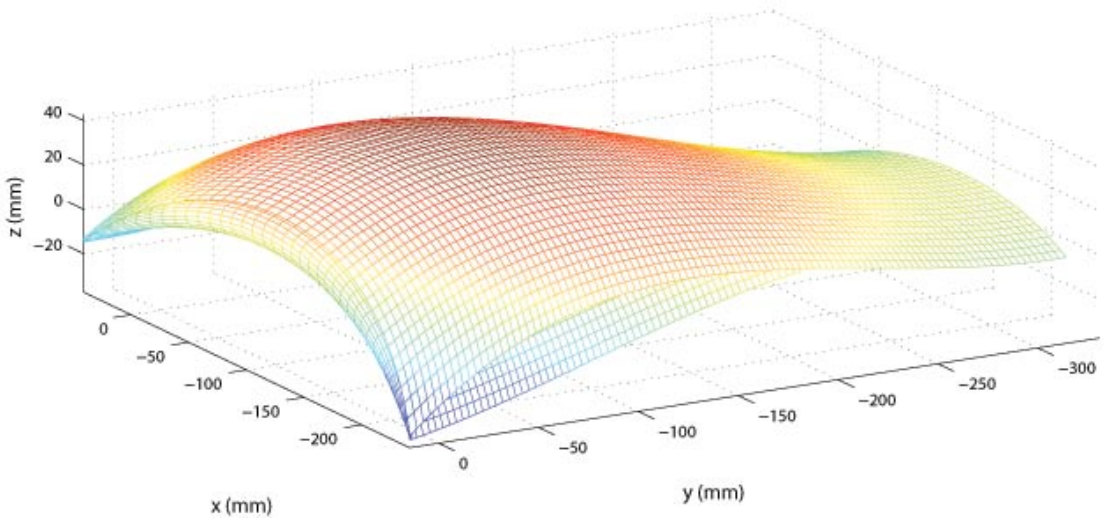

Figure 8. Three-dimensional wing reconstruction. Regression techniques are used to fit surface polynomials and leading edge is fitted using a Bezier function. The trailing edge is given a thickness of 1mm based on measurements of the eagle's feathers.

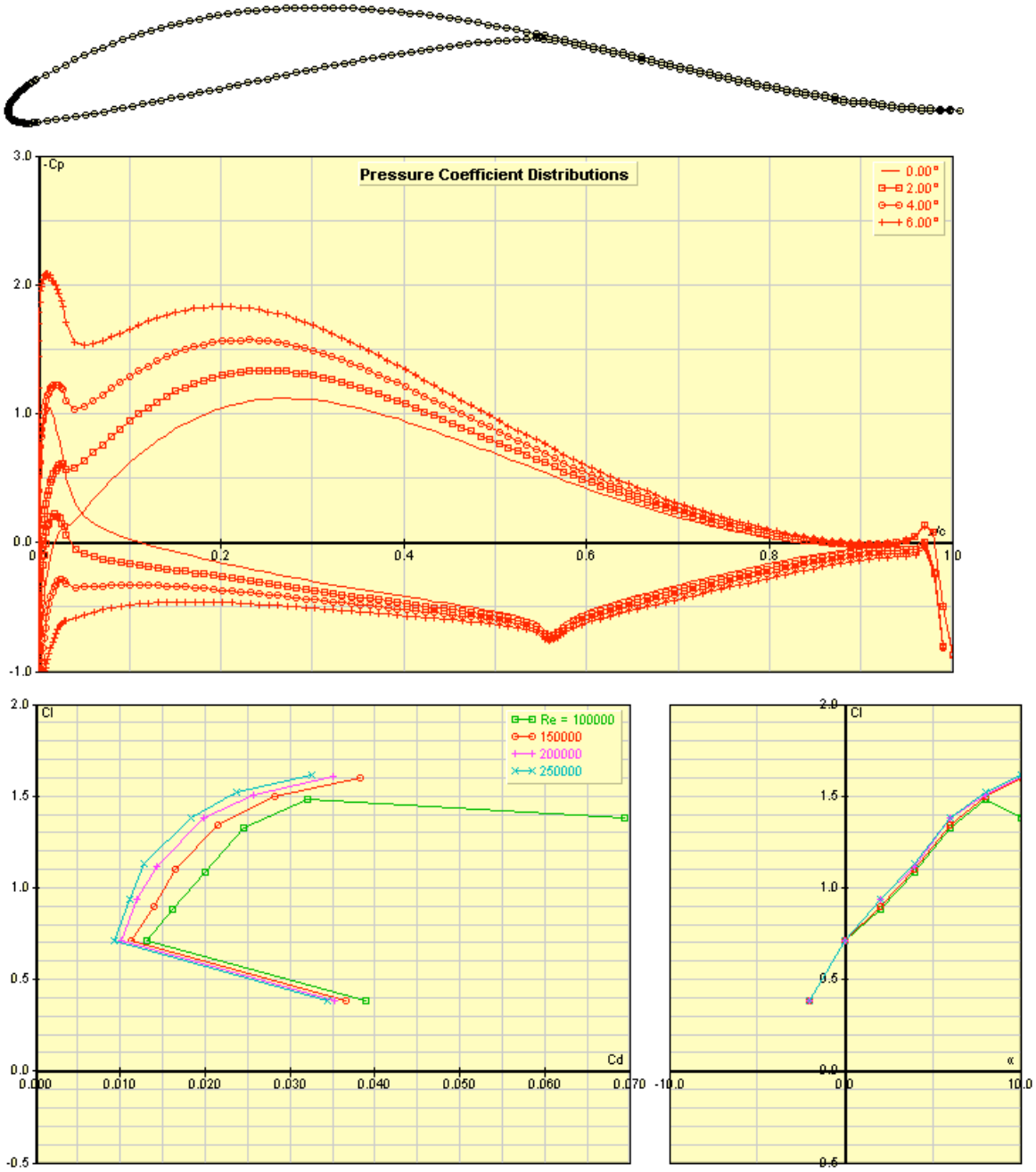

Figure 9. Javafoil results for airfoil section taken at half span with added 1mm thickness trailing edge. The results are only expected to be reliable in the region of 0<α<8º.

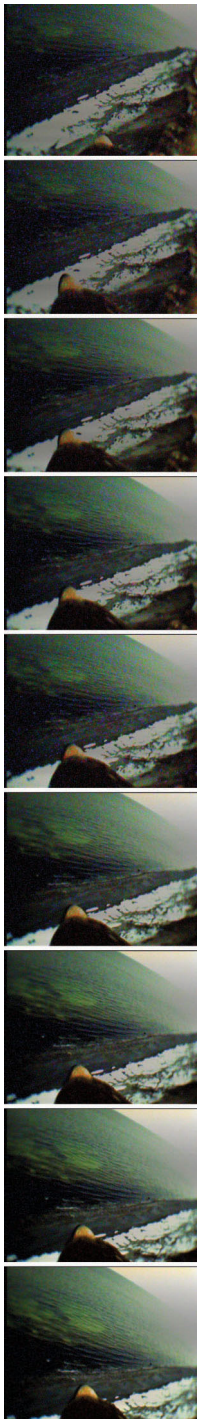

Figure 10. Onboard video sequence of head nystagmus during a banked turn. Note the fast saccadic head movement in the first two frames, which is followed by a period of gaze fixation in the remaining frames.